

Calibration Techniques for VERITAS

David Hanna[1] for the VERITAS Collaboration[2]
[1] *Physics Department, McGill University, 3600 University Street, Montreal, QC H3A 2T8, Canada*
[2] *For full author list see G. Maier "VERITAS: Status and Latest Results", these proceedings*
hanna@physics.mcgill.ca

arXiv:0709.4479v1 [astro-ph] 27 Sep 2007

Abstract: VERITAS is an array of four identical telescopes designed for detecting and measuring astrophysical gamma rays with energies in excess of 100 GeV. Each telescope uses a 12 m diameter reflector to collect Cherenkov light from air showers initiated by incident gamma rays and direct it onto a 'camera' comprising 499 photomultiplier tubes read out by flash ADCs. We describe here calibration methods used for determining the values of the parameters which are necessary for converting the digitized PMT pulses to gamma-ray energies and directions. Use of laser pulses to determine and monitor PMT gains is discussed, as are measurements of the absolute throughput of the telescopes using muon rings.

Introduction

Like all gamma-ray detectors which use the atmospheric Cherenkov technique, the VERITAS instrument is fundamentally quite simple. Each of its four telescopes consists of a 12 m reflector which directs Cherenkov light from air showers onto a matrix of 499 photomultiplier tubes (PMTs) which are read out using 500 MSample/s flash-analog-to-digital converters (FADCs). In order to translate the digital information emerging from the FADCs into a form which can be used to select gamma-initiated showers from background and determine the energy and direction of the incident gamma ray, one needs calibration constants. These 'constants' (which are not, strictly speaking, constant) need to be determined when commissioning the detector and monitored and adjusted periodically during the lifetime of the project. In this paper we describe techniques employed by the VERITAS collaboration to accomplish this task; two techniques use a laser to determine the absolute gains of the PMTs and one uses Cherenkov images, generated by isolated muons, for inter-telescope calibration and determination of absolute throughput. Some of these issues are addressed independently with a remote LIDAR-like system described elsewhere in these proceedings [1].

The VERITAS Laser System

For flat-fielding and gain monitoring, VERITAS uses a nitrogen laser (λ = 337 nm, pulse energy 300 μJ, pulse length 4 ns). The beam is sent through neutral density filters arranged in two sequential wheels, with 6 filters each, such that transmissions ranging from less than 0.02% to 100% may be chosen. It is then divided, approximately equally, among 10 optical fibres, four of which are routed to opal diffusers located on the optical axes of the telescopes, 4 metres from the PMTs in the cameras. A fifth fibre supplies light to a PIN photodiode to provide a fast external trigger for FADC readout; self-triggers using only PMT information are also used for some applications. There is, at present, no independent monitor for measuring the pulse-to-pulse fluctuations in the laser intensity (typically 10%); these are monitored using a sum over a large number of PMTs in each camera.

Nightly Laser Runs

A five-minute, 10 Hz laser run at nominal intensity is taken at the beginning of each observing night. The data obtained are used primarily for monitoring gain evolution and checking for problems. Other tests, described below, are done less frequently. Since the opal diffuser spreads the laser light uniformly (to better than 1%) over the face of the camera, the pulses can be used for flat-fielding the response of the channels. The high voltages of the individual PMTs are adjusted so that the average pulse size in each channel is the same for all channels. A PMT's average pulse size depends on the product of its photocathode's quantum efficiency and the efficiency for photoelectrons to be collected by its first dynode, as well as on the gain in the electron multiplier stage. To a lesser extent it depends on the reflectivity of the Winston-cone light concentrator in front of each PMT. The average pulse sizes are calculated and written to a database for use in off-line analysis.

The gain of the electron multiplier can be tracked separately using the daily laser data using the method of photostatistics. In this method, we remove laser fluctuations using a sum-over-PMTs monitor and the effects of electronics noise and night sky background are measured in runs with zero laser intensity and unfolded. Then, to first order, we can state that the mean charge in a laser pulse is given by $\mu = GN_{pe}$ with G the gain and N_{pe} the mean number of photoelectrons arriving at the first dynode. Assuming that only Poisson fluctuations in N_{pe} determine the width, σ, of the charge distribution, we have $\sigma = G\sqrt{N_{pe}}$. Thus we can solve for gain as $G = \sigma^2/\mu$. Taking into account statistics at the other dynodes, which are in general described by a Polya distribution, leads to a correction factor such that $G = \sigma^2/\mu/(1+\alpha^2)$ where α is the width parameter which would result from injecting only single photoelectrons into the dynode chain. For our PMTs and their associated dynode voltages we simulate $\alpha = 0.47$, which results in a revised estimate for multiplier gain of $G' = 0.82\ \sigma^2/\mu$.

As a check on this model, note that $\mu = G'N_{pe}$ or $N_{pe} = \mu/G'$. This quantity is plotted for a representative PMT, in figure 1, as a function of applied high voltages in steps from nominal HV. Except perhaps for an effect due to increased first dynode collection efficiency due to increased HV, we do not expect N_{pe} to change and the plot shows that it is constant over the

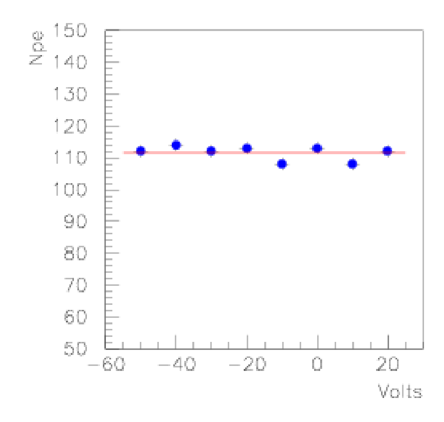


Figure 1: Mean number of photoelectrons captured by the first dynode of a representative PMT *vs* deviation from its nominal high voltage setting. The flat line is to guide the eye and emphasize that there is no significant change.

Single Photoelectrons

An alternative method for determining PMT gain is to directly measure the position of the single photoelectron peak in a pulse size spectrum. Again, this gives the gain of the electron multiplier structure (and any downstream electronics) and does not include effects of the photocathode. To resolve the single photoelectron peak, we take special laser runs at very low intensity where the average number of photoelectrons resulting from each laser pulse is less than 1.0. The resulting spectrum consists of a pedestal, the single photoelectron peak, and small admixtures of two, three *etc* peaks with the relative sizes of each component prescribed by Poisson statistics. We also rely on the constraint that the multi-photoelectron signals can be fit with the same parameters (mean and width) as the single photoelectron peak (up to

multiplicative factors). Allowing only a small number of free parameters results in robust fits to the spectra, an example of which is shown in figure 2. In this example the relative width of the single photoelectron peak is found to be 0.48. The average from a group of channels is 0.47. The data for this study were obtained using twice the normal gain, in order to resolve more clearly the single photoelectron peaks. With such a gain the simulation predicts a relative width of 0.44.

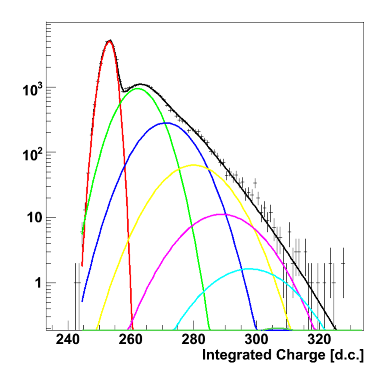


Figure 2: A pulse size spectrum made with highly attenuated laser pulses and raised high-voltage. The single photoelectron peak is clearly visible as the structure next to the pedestal, which is the dominant feature. The data are fit with a sum of Gaussians as described in the text.

In order to maintain good signal-to-noise for this measurement, we cover the camera with a thin aluminum plate with a 3 mm hole drilled at the location of the centre of each PMT. This reduces the night sky background to the point where it is negligable compared with the laser light. Indeed, with the telescope in stow position, one can perform single photoelectron laser runs in the presence of moonlight. This is an important consideration given that sufficient statistics (~50000 shots) require nearly an hour of running.

The gain values which result from the method of photostatistics and from the single photoelectron fitting are in units of digital counts per photoelectron. A comparison of the two methods is shown in figure 3 where results from telescope 1 are shown.

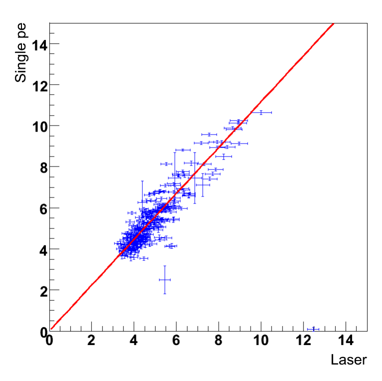


Figure 3: A comparison of gains determined using photostatistics (abscissa) with those determined from single photoelectron fitting (ordinate). The slope of the correlation is approximately 1.1. It should be 1.0; the discrepancy is an indication of the present scale of the systematic error of the gain-measuring procedures.

The data points in this figure highlight the difference between the 'multipler gain', which includes everything starting from the first dynode, and the 'overall gain' which also includes the light concentrator cones and the photocathodes. Since the PMTs have all been flatfielded according to the overall gain, the dispersion seen along the correlation line in figure 3 is due to channel-to-channel differences in these 'front end' components.

Muon Rings

Local muons are normally a nuisance for Cherenkov telescopes but they can be useful in providing a measurement of the optical throughput of the detector [3, 2]. Muons passing through the centre of the telescope with trajectories parallel to its optical axis will produce azimuthally symmetric rings in the camera. The rings will have radii given by the Cherenkov angle of the muons (maximum value about 1.3 degrees) and the total number of photons expected in the ring can be calculated from the measured value of this angle.

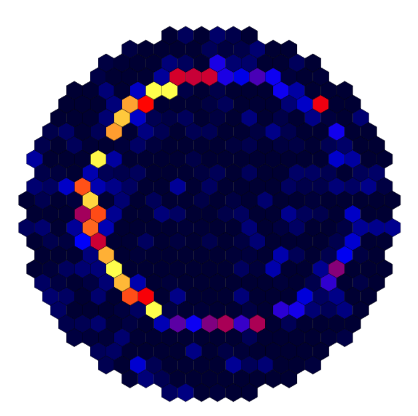


Figure 4: A muon image recorded by VERITAS telescope 1. Pulse size in each PMT is colour-coded - the azimuthal nonuniformity is the result of a non-zero impact parameter.

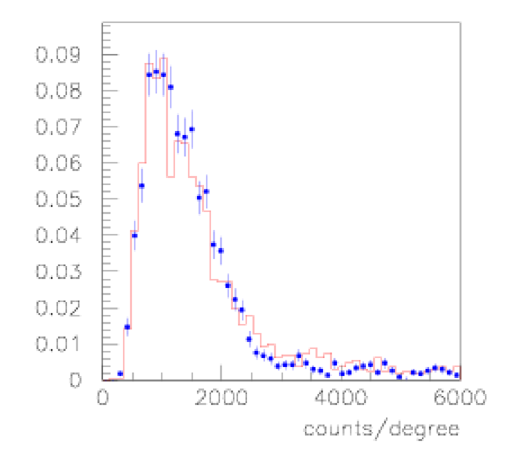


Figure 5: Detected charge in muon arcs, normalized to their lengths, for VERITAS telescopes 1 (histogram) and 2 (data points), showing that they are well matched.

Muons with non-zero impact parameters will produce arcs with an azimuthally dependent photon density and muons arriving at an angle with respect to the telescope's axis will give rise to arcs with centres that are offset from the centre of the camera.

Muon ring images can be obtained from normal data where they occur as part of hadronic showers. The images are cleaned (channels are required to have a minimum pulse size and to be next to other channels with non-zero charge, otherwise they are set to zero) and a ring is fit to the image. Further cleaning of the images, where charge deposits far from the fitted ring are suppressed, removes light from other components of the shower of which the muon was a member. After this second cleaning the ring parameters are re-calculated. A cleaned image of a complete muon ring is shown in figure 4.

Since the morphology and location of the muon ring allow the muon's trajectory to be calculated, it is possible to predict with precision the number of Cherenkov photons that should be collected by the camera. This requires knowing the reflectivity of the mirror facets, shadowing effects due to the camera support structure, *etc* so the detector response to local muons is a good check on our understanding of the instrument. Absolute calculations are still in progress but certain relative measurements have already been implemented, such as inter-telescope calibration and month-to-month stability checks. An example is shown in figure 5 where we histogram the summed charge in each muon arc, divided by its length, for two telescopes in the array. The overlap of the two histograms, normalized by the number of entries, shows that the telescopes are well balanced.

Acknowledgements

This research is supported by grants from the U.S. Department of Energy, the U.S. National Science Foundation, and the Smithsonian Institution, by NSERC in Canada, by PPARC in the UK and by Science Foundation Ireland.

References

[1] M. Hui et al. *these proceedings*.

[2] T. B. Humensky et al. *Proc. 29th ICRC, Pune*, 2005.

[3] G. Vacanti et al. *Astropart. Phys.*, 2:1–11, 1994.